View metadata, citation and similar papers at core.ac.uk
brought to you by CORE
provided by JEOS:RP - Journal of the European Optical Society Rapid publications

Refractive index determination of SiO_2 layer in the UV/Vis/NIR range: spectrophotometric reverse engineering on single and bi-layer designs

L. Gao Beijing Institute of Technology, Beijing, China

F. Lemarchand Institut Fresnel, Aix Marseille Université - Ecole Centrale Marseille - CNRS, UMR 7249, 13397 Marseille, France
fabien.lemarchand@fresnel.fr

M. Lequime Institut Fresnel, Aix Marseille Université - Ecole Centrale Marseille - CNRS, UMR 7249, 13397 Marseille, France

In this paper we use spectrophotometric measurements and a Clustering Global Optimization procedure to determine the complex refractive index of SiO_2 layer from 250 nm to 1250 nm. A special commercial optical module allows the reflection and transmission measurements to be made under exactly the same illumination and measurement conditions. We compare the index determination results obtained from two different single layer SiO_2 samples, with high and low index glass substrates, respectively. We then determine the refractive index of SiO_2 for a bi-layer design in which the first deposited layer is Ta_2O_5. The corresponding solutions are discussed and we show that the real part of the complex refractive index obtained for a bi-layer is slightly different to that found for a single layer investigation. When SiO_2 is included inside a thin film stack, we propose the use of an index determination method in which a bi-layer is used for the real part of the complex refractive index, and single layer determination is used for the imaginary part of the refractive index in the UV range. [DOI: http://dx.doi.org/10.2971/jeos.2013.13010]

Keywords: SiO_2 thin film, optical properties, refractive index determination

1 INTRODUCTION

The determination of the complex refractive index (refractive index n and extinction coefficient k) of thin films is of great importance for the design and production of any optical interference filters. Successful manufacturing of such filters is often directly related to the accuracy of the complex refractive index and thickness (d) measurements, since even a small difference in refractive index can lead to drastic changes in the filters spectral response (reflectance R and transmittance T). Moreover, the index of thin films, which differs from that of bulk materials, strongly depends on the deposition techniques and conditions. The index of a single layer can also change in a multilayer structure, because the deposition conditions, especially temperature, vary with time [1]. Therefore, the determination of the complex refractive index and thickness, which can be considered to be a reverse engineering process, is clearly necessary.

The determination of these optical parameters and thicknesses is generally carried out by means of ellipsometric and spectrophotometric analysis. Due to the complicated nature and high cost of the ellipsometer, more readily available and affordable spectrophometer has attracted considerable attention.

In the case of spectrophotometric analysis, the envelope method, using the envelopes of the oscillating transmittance or reflectance spectra, was developed many years ago. This method does not require any postulate or assumptions with respect to the optical dispersion model. Manifacier [2] and Swanepoel [3, 4] have improved this method, in order to determine the optical parameters and thickness of a non-absorbing or weakly absorbing single layer, deposited onto a transparent or weakly absorbing substrate. An alternative solution for a weakly absorbing layer consists in analysing the spectral wavelengths corresponding to reflectance extremes, at several oblique angles of incidence [5]. An error minimization method [6] and a midpoint method [7] have also been proposed. However, the accuracy of this approach still strongly depends on the definition of these envelopes. In addition, this method does not work for film having significant dispersion and/or strong absorption. The other technique based on spectrophotometric analysis is the curve fitting method, which requires an optical dispersion model. This model is able to integrate a considerably greater quantity of spectral information, such as transmittance and reflectance, or spectra at multiple oblique incidences, into the index determination process [8]. In addition, it is also able to manage complicated cases, such as strongly absorbing and complex multilayer filters.

As SiO_2 is the mostly commonly used low index film in many types of multilayer interference coatings, the determination of its refractive index, which can be essential to the successful production of a high quality multilayer filter, should be carefully investigated. In the present paper, we study three different configurations for the determination of the refractive index of SiO_2, using the curve fitting method in the UV/Vis/NIR range. A SiO_2 layer was deposited onto a low

Received July 02, 2012; revised ms. received November 23, 2012; published January 31, 2013 ISSN 1990-2573

index Corning 7980 Fused Silica substrate [9] and a high index S-LAH66 substrate [10]. In this present study, a bi-layer Ta_2O_5/SiO_2 was also deposited onto a fused silica, following a procedure proposed in [11] where a bi-layer was deposited in order to overcome the problem of less contrast of interference fringes. Then, from spectrophotometric measurements at quasi-normal incidence, we tried to determine the complex refractive index and thickness for these three configurations, using a Clustering Global Optimization algorithm. We discuss this method, the results, the accuracy and the limitations of these three configurations. The layers were assumed to be homogeneous. Some authors [12] have pointed out that by taking the inhomogeneities into account, the index determination can be substantially improved if the fit between the theoretical (homogeneous model) and experimental data is poor. In the case of a single layer, the inhomogeneities can be easily detected, by comparing the minimum reflectance values with that of the bare substrate.

2 THEORETICAL ANALYSIS: INFLUENCE OF THE SUBSTRATE'S REFRACTIVE INDEX ON THE SiO_2 SINGLE LAYER INDEX DETERMINATION

The refractive index determination of a single layer, by means of spectrophotometric measurements can be performed easily under certain conditions:

- The internal transmittance of the substrate should be very close to 100%. Otherwise, it is very difficult to distinguish the absorption produced by the layer from that produced by the substrate. A 1 mm thick UV grade fused silica substrate classically presents an internal transmittance in excess of 99.9% at wavelengths above 250 nm. The same transmittance should be found for a S-LAH66 substrate at wavelengths above 420 nm.
- The layer should not be opaque. When the transmittance approaches zero, many different solutions (n, k) can fit the experimental reflectance data.
- The films inhomogeneities should be evaluated. In the case of a transparent or weakly absorbing film, these can be checked by measuring the reflectance at wavelengths (λ) for which $nd = p\lambda/2$ where p is an integer.
- The accuracy of measurements is of prime importance. A systematic measurement error leads to an incorrect index determination, depending on the sensitivity of the layers index to the photometric measurements. This last point deserves further discussion. In the case of a transparent film, its transmittance (or reflectance) is characterized by interference fringes, the extreme values of which can be expressed as [3]:

$$T_{HW} = \frac{2n_s}{n_s{}^2 + 1} \tag{1}$$

$$T_{QW} = \frac{4n^2 n_s}{n^4 + n^2(n_s{}^2 + 1) + n_s{}^2} \tag{2}$$

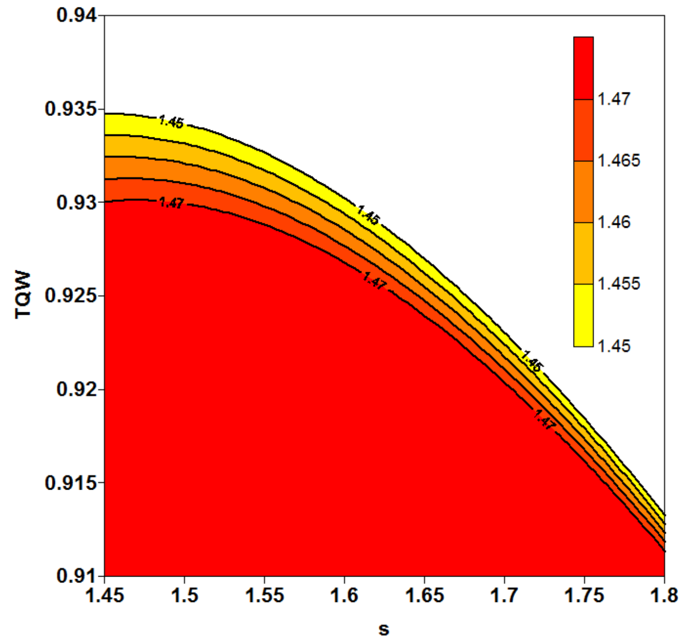

FIG. 1 Layer index as a function of T_{QW} and the substrate index, i.e., $n = f(T_{QW}, n_s)$.

where n_s is the substrate refractive index, T_{HW} and T_{QW} are the T values reached for a half wavelength combination: $nd = p\lambda/2$, and for a quarter wavelength combination: $nd = (2p+1)\lambda/4$, respectively (where p is an integer).

Clearly, the T_QW values are the signature of the layers index, and shifts in the values of T_{QW} lead to shifts in the value of the layers refractive index. In the case of a single SiO_2 layer, depending on the wavelength, the layer index lies in the approximate range: n =1.45∼1.5. Using Eq. (2), one can extract the layer index n as a function of n_s and T_{QW}. Figure 1 illustrates the relationship among the layer index n (plotted values), T_{QW} (vertical axis) and the substrate index (horizontal axis). We then define the layer index sensitivity S (n,n_s) as the layer index shift corresponding to a small variation of T_{QW}, for a given substrate index, as expressed by Eq. (3):

$$S(n, n_s) = \left(\frac{\partial n}{\partial T_{QW}}\right)_{n_s fixed} \tag{3}$$

As shown in Figure 1, for a substrate index equal to 1.45 a variation in T_{QW} of approximately 0.005 (from 0.93 to 0.935) leads to a shift in layer index of 0.02 (from 1.47 to 1.45), and $S(1.45, 1.45) = 4$. For comparison, $S(1.45, 1.78) = 8$.

The inaccuracy of the photometric measurements is generally $\Delta T = 0.001$ [13, 14], which leads to an uncertainty in the layer index of approximately 0.004 for the case of a fused silica substrate ($n_s = 1.45$) and 0.008 for a S-LAH66 substrate ($n_s = 1.78$). This outcome therefore favors the use of a low index substrate, although the low contrast of interference fringes can make it difficult to determine the thickness. This will be illustrated in Figure 3.

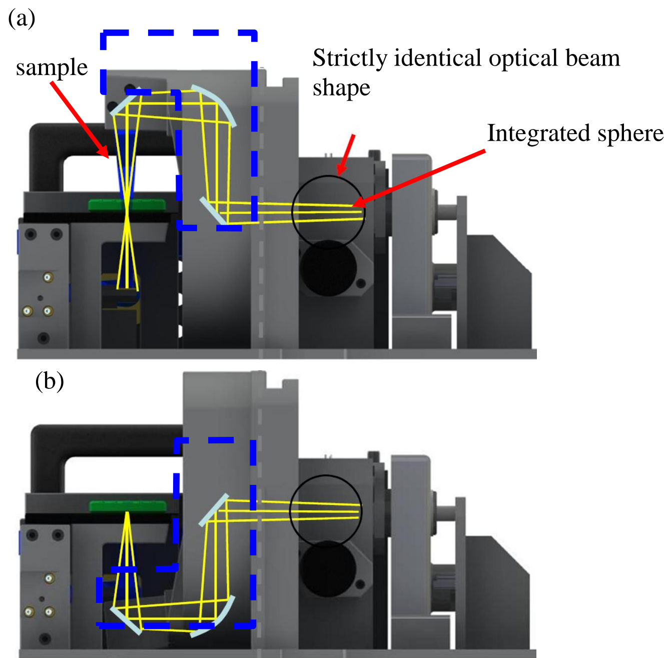

FIG. 2 OMT module for transmittance (a) and reflectance (b) configurations. The moving part, consisting of three reflecting mirrors, is indicated by the dashed lines.

3 EXPERIMENTAL SETUP AND SPECTRAL MEASUREMENTS

We used a commercial Perkin Elmer lambda 1050 spectrophotometer with a specific module developed by OMT Solutions, as shown in Figure 2. The sample is placed horizontally, with the same measurement spot used for both reflectance (R) and transmittance (T) at quasi-normal angle of incidence (8°). The incident beam presents a divergence below 1 degree, and a calculation considering a perfected collimated beam is sufficient in almost cases. The illuminated zone on the sample is a square of 2mm side. The switchover between R and T configurations is performed automatically by means of a 180° rotation of the detection system. An integrating sphere measures the reflected/transmitted flux from 250-2500 nm. Both the incident beam and the detection system are similar for the R and T configurations, such that it makes sense to estimate the samples absorbance (A) using: $A = 1\text{-}R\text{-}T$.

In the present study, three samples were deposited using the ion assistance electronic beam deposition technique. This technology is able to produce very high-density layers, with stable optical properties close to those of bulk materials. We deposited a single SiO_2 layer with a thickness of approximately 300 nm onto fused silica (sample S1) and S-LAH66 (sample S2) substrates. Then, a bi-layer Ta_2O_5/SiO_2 film was deposited onto fused silica (sample S3). We restricted the experimental spectral range to 250-1250 nm for the samples with a fused silica substrate, i.e., S1 and S3, and to 420-1250 nm for the S-LAH66 substrate, i.e. S2, and used a 2 nm measurement interval. The experimental reflectance (Rexp), transmittance (Texp) and absorbance of these samples are plotted in Figure 3. The theoretical values of bare SiO_2 and S-LAH66 substrates are also shown.

As shown in Figure 3(a) and 3(b), for sample S1 the spectral oscillations are barely visible, and |THW-TQW| lies in a range close to 0.5%, whereas the oscillations are clearly visible for sample S2, with |THW-TQW| lying in a range close to 6%. This difference in oscillation amplitudes is due to the different contrasts in refractive index between the substrate and the layer. The spectral responses of S3 are characterized by many oscillations, which in fact contain 'considerable information' related to the bi-layer design. In some spectral regions, its transmission is greater than that of the bare substrate, thus correspond-

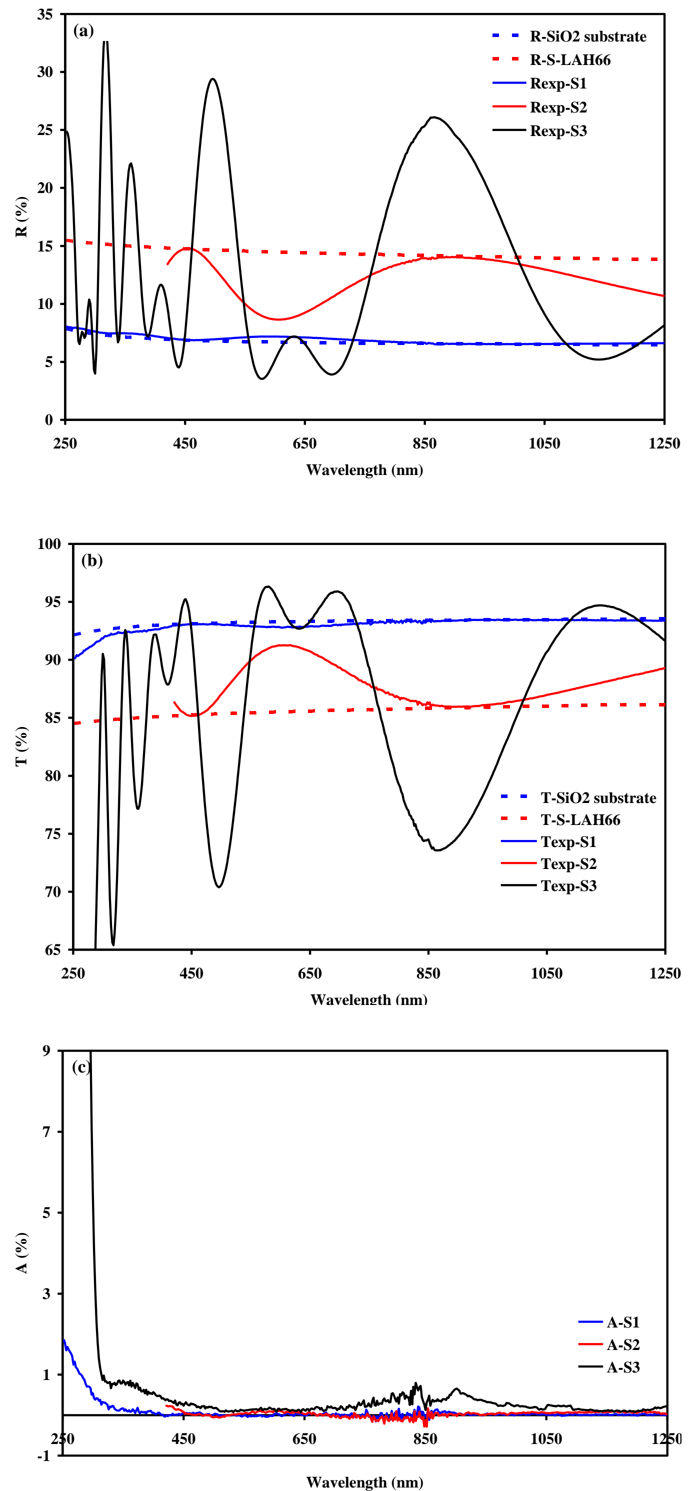

FIG. 3 Experimental reflectance (a), transmittance (b) and absorbance (c) of sample S1, S2, S3, and theoretical values for a bare SiO_2 substrate and a bare S-LAH66 substrate in (a) and (b), as a function of wavelength.

ing to the local production of an anti-reflection effect, and in other regions the opposite effect is produced.

Figure 3 shows that the absorbance is not detectable for sample S2, since the measurements begin at 420 nm on the S-LAH66 substrate. In the case of samples S1 and S3, their absorbance typically decreases when the wavelength increases from 250 nm to a certain cutoff wavelength λ_S. Above λ_S, the absorbance is not detectable. From these absorbance curves, λ_{S1} can be estimated to be approximately 330 nm, i.e., shorter than λ_{S3} (about 450 nm), even in the presence of measurement noise of approximately 0.2% over the range [250-700 nm], and 0.5% at wavelengths above 750 nm. The value of λ_S is directly related to the lowest energy gap of the materials inside a thin film stack. As the bi-layer includes SiO_2 and Ta_2O_5, and the energy gap of Ta_2O_5 is known to be below that of SiO_2 [15, 16], the starting absorption wavelength of S3 is longer than that of S1. At short wavelengths, the absorbance of S3 is contributed mainly by the Ta_2O_5. It can thus be concluded that k (SiO_2) is undetectable for $\lambda > \lambda_{S1}$, whereas k (Ta_2O_5) is undetectable for $\lambda > \lambda_{S3}$.

4 COMPUTATIONAL PROCEDURE FOR THE INDEX DETERMINATION

The complex refractive index of a thin film is estimated from the reflectance and transmittance values, as shown in Figure 4. The theoretical reflectance (Rcal) and transmittance (Tcal) were calculated using the matrix method [17], taking the backside reflectance into account. They depend on the measurement wavelength, the refractive index of the substrate n_s, the complex refractive index (n, k), and the thickness (d) of the layer. n_s was assumed to be known. Accordingly, the complex refractive index and thickness of the layer need to be determined.

There are several optical dispersion models describing the laws of the complex refractive index. The most frequently used is Cauchy, which is simple and performs well for a transparent thin film. As wavelengths as short as 250 nm were used in this study, the thin SiO_2 - Ta_2O_5 film exhibits absorption, and the Tauc-Lorentz model (TLM) [18] is then more suitable. TLM, which has been widely used for many amorphous materials [19]–[21], was derived from the Tauc joint density of states. The standard Lorentz form for the imaginary part of the dielectric function (ϵ_2) of a set of oscillators [22] is given by:

$$\epsilon_2(E) = \begin{cases} \frac{AE_0C(E-E_g)^2}{(E^2-E_0{}^2)^2+C^2E^2}\frac{1}{E} & (E > E_g) \\ 0 & (E \leq E_g) \end{cases} \tag{4}$$

where E_g is the band gap, E_0 is the peak transition energy, C is a broadening parameter and A is a factor representing the optical transition matrix elements.

The real part of the complex dielectric function (ϵ_1) can be retrieved from the Kramers-Kronig relation [23], thus introducing another free parameter ϵ_∞.

Since

$$E = \frac{hc}{\lambda} \tag{5}$$

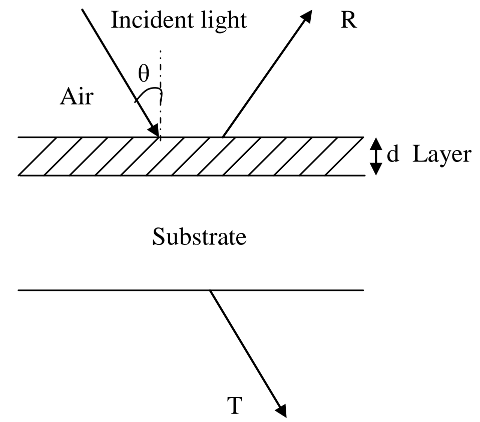

FIG. 4 Optical characteristics of a thin film coating on a substrate.

where h is Planck constant and c is the speed of light, Eq. (4) can be rewritten in order to express ϵ_2 and ϵ_1 as a function of λ.

Since

$$\epsilon_1 - i\epsilon_2 = (n - ik)^2 \tag{6}$$

the refractive index n and the extinction coefficient k can then be derived.

Six parameters are thus required in order to fully characterise a single layer (E_g, A, E_0, C, ϵ_∞ and d), and twelve parameters are needed for a bi-layer. An error function (EF) was used to denote the difference between the calculated and experimental reflectance or transmittance values:

$$EF(X,d) = 0.5\sqrt{\frac{1}{N_w}\sum_{j=1}^{N_w}\left(\frac{R_j(X,d) - R_{j,exp}}{\Delta R_j}\right)^2} + 0.5\sqrt{\frac{1}{N_w}\sum_{j=1}^{N_w}\left(\frac{T_j(X,d) - T_{j,exp}}{\Delta T_j}\right)^2} \tag{7}$$

where N_w is the number of wavelengths. For each value of j, R_j and T_j are respectively the computed values of reflectance and transmittance, whereas $R_{j,exp}$ and $T_{j,exp}$ are the experimental values of reflectance and transmittance, and d is the thickness of the film. X is a vector containing the free parameters derived from the laws governing the refractive index n and the extinction coefficient k. ΔR_j and ΔT_j are respectively the uncertainties on the values of reflectance and transmittance (in this paper $\Delta R_j = \Delta T_j = 1$, which makes sense with our measurement system where reflectance and transmittance are measured with the same accuracy).

As a consequence of the relatively large number (12) of variables required to compute the EF, a simple local non-linear least-squares optimisation technique is inefficient, and a global optimization procedure is required. In the global optimization process, EF is considered to be the objective function for which the global minimum must be found. As reported in our previous study [24], the Clustering Global Optimization (CGO) algorithm [25, 26] performs perfectly for the determination of the complex refractive index and thickness of thin films. The underlying principle of this

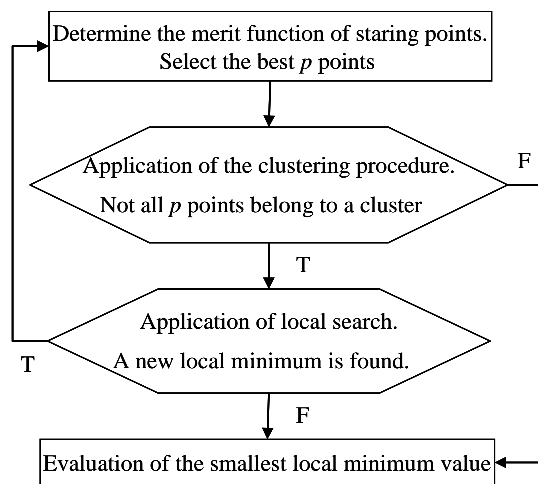

FIG. 5 CGO flowchart.

method, which has demonstrated its efficiency in solving thin-film design problems, is recalled below [27]–[29].

CGO methods can be viewed as a modified form of the standard Multistart procedure, in which a local search is performed from several starting points distributed over the entire search domain. A drawback of the Multistart technique is that when a large number of starting points is used, the same local minimum may be identified several times, thereby leading to an inefficient global search. Clustering methods are designed to avoid this inefficiency, through careful selection of the points from which the local search is initiated.

As shown in Figure 5, the CGO algorithm can be described as follows:

(1) Consider m points with a uniform distribution, in an initially n-dimensional space, and add them to the current sample *CS*. Then refine this distribution to a smaller selection of only p points in *CS*, having the best merit function.

(2) Apply the clustering procedure to these p points. If all of the points belong to a cluster, go to step (4). Let p be the number of non clustered points.

(3) A local search is applied to these p points. If a new local minimum is found, go to step (1): with m new starting points surrounding the local minimum.

(4) Find the local minimum having the smallest value.

As step (3) allows a new starting process to be initiated in the vicinity of the previous local minimum, the local procedure can find solutions outside the starting interval. This characteristic of the algorithm led us to refer to it as a “global optimization procedure”, even though the global aspect is not demonstrated.

Taking a simple 1-dimensional function as an example, the functioning of the CGO can be more easily understood, as shown in Figure 6. Each step is described:

(1) The aim is to find the global minimum after comparing all the local minima of a function. In the present drawn case, three minima exist (x = 5.1, x = 8.2 and x = 11).

(2) Choose a starting interval x ∈ [4-8] and a density grid (m = 9 points). Select the p best evaluated points (p = 6 points).

(3) A local descent is applied to the best p evaluated points. Two local minima are thus detected (x = 5.1 and x = 8.2).

(4) Perform a new local search with new starting intervals in the vicinity of the two local solutions: a new local minimum is detected (x=11). The interesting fact is that this new solution does not belong to the initial starting interval x ∈ [4-8].

(5) A new starting interval is imposed around the new minimum. When all local searches lead to the already detected solutions, the global minimum is found by comparing all of the local minima, and the algorithm is then stopped.

The efficiency of CGO depends on the starting interval: with a small starting interval it is difficult to jump to another minimum. With a given density grid, a broader starting interval leads to a larger step between evaluated points. Under such conditions, the program may be unable to detect very sharp minimum peaks. A good compromise, which can be found with the users experience, is mandatory when a high number of variables (typically $>$ 20) is used, and one can expect to find all of the minimum values in cases where the number of variable parameters is less than 20. Of course, for problem where solutions are not perfectly known, one does not have proof that the global minimum is detected by CGO. By changing either starting interval or grid density or number of selected points, one may check that the global solution remains constant, which is a beginning of proof.

5 RESULTS AND DISCUSSION

CGO provides a unique solution, with an excellent EF value (below 0.1) for both S1 and S2 problems. The number of starting points is set to m = 1000, and the number of p minimum is set to 10. These values are chosen from our experience on an optimization problem with 6 variables describing n,k and d. The optimized parameters E_g, E_0, C, A, ϵ_∞ and d allow n and k to be computed.

The corresponding values for samples S1 and S2 are plotted in Figure 7. Concerning n, the values are nearly identical, with differences smaller than 10^{-4}. Concerning k, it appears that for wavelengths in the range [420-450 nm], SiO_2 is absorbant for S2. We are convinced that if S2 is slightly absorbing, this is due to the internal transmittance of the S-LAH66 substrate, which begins to be lower than 1. Under this assumption, k cannot be detected on a S-LAH66 substrate. Conversely, the fused silica substrate allows k to be determined over the range [250-330 nm]. We determined the value of k to be 10^{-3} at λ = 260 nm. For wavelengths above 330 nm, k is smaller than 2 $\cdot 10^{-4}$. We consider this to be the minimum threshold value that can be extracted from our spectrophotometric determination. Moreover, for values of k of the order of 10^{-4}, other

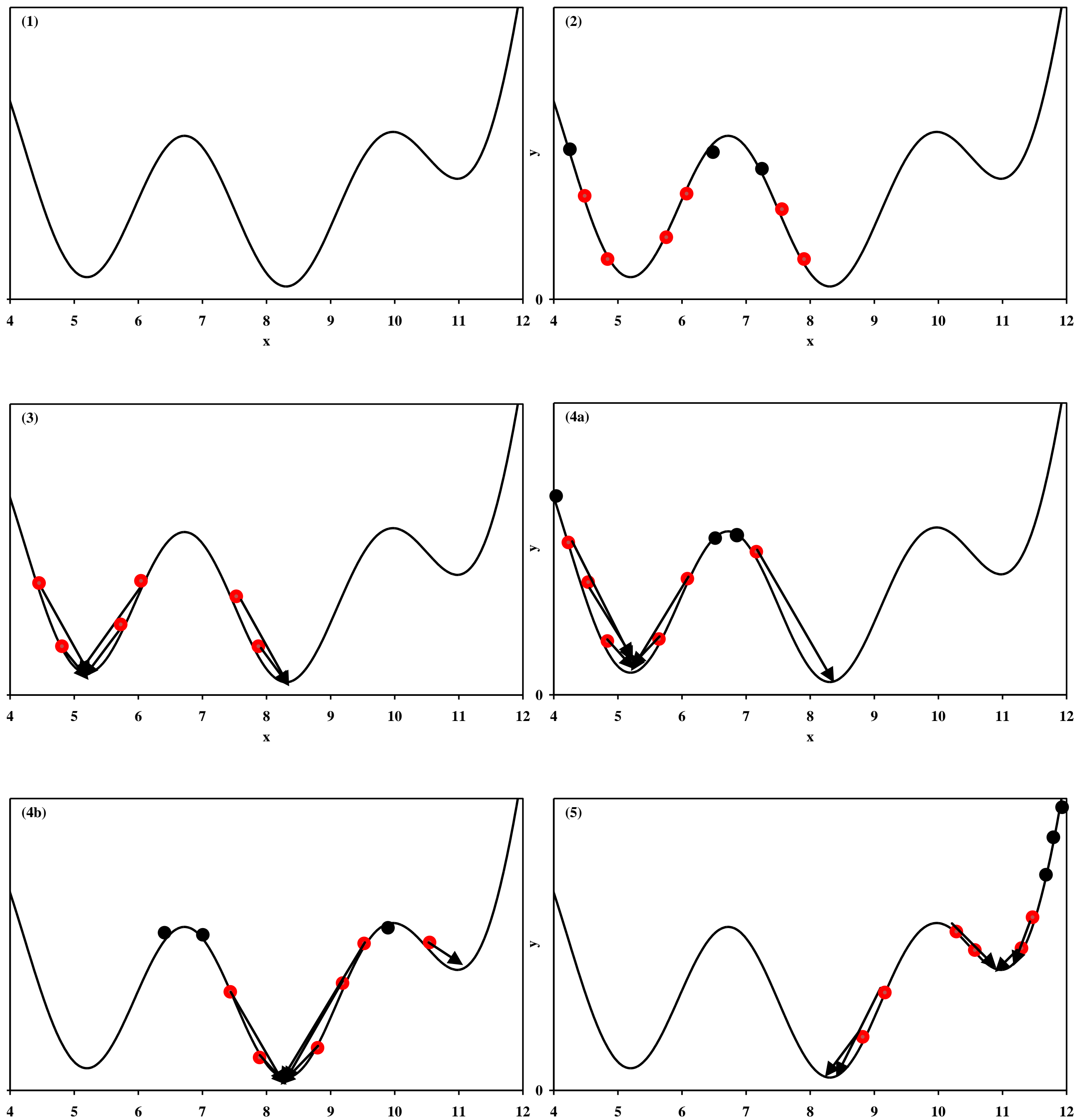

FIG. 6 Example of a 1-dimensional function illustrating the functioning of CGO.

techniques such as Cavity Ring-down Spectroscopy [30] are better adapted.

For the S3 – bi-layer design investigations, we tested two configurations:

Config. (a): all parameters, i.e., thicknesses, real and imaginary parts of the complex refractive index (12 parameters) were made variable. This configuration confers a high flexibility to all of the parameters. CGO provides one solution (sol1) for this configuration.

Config. (b): this configuration is proposed as a consequence of the difficulty in determining $k(SiO_2)$, since it is likely that most of the absorption is produced by the Ta_2O_5 layer. We then chose to set $k(SiO_2)$ to the value obtained from the S1 optimization. All of the other parameters remained variable. CGO provides two solutions (sol2 and sol3) for this configuration.

The EF values of the three solutions are very similar, i.e., EF ≈ 0.32. For the purposes of illustrating the curve-matching achieved with this method, Figure 8 shows a plot of the fit between the experimental and calculated spectra of sol1. As suggested by their similar EFs, the fits of sol2 and sol3 are also satisfactory. For the refractive index of the Ta_2O_5 layer, the three solutions lead to a satisfying value, consistent with

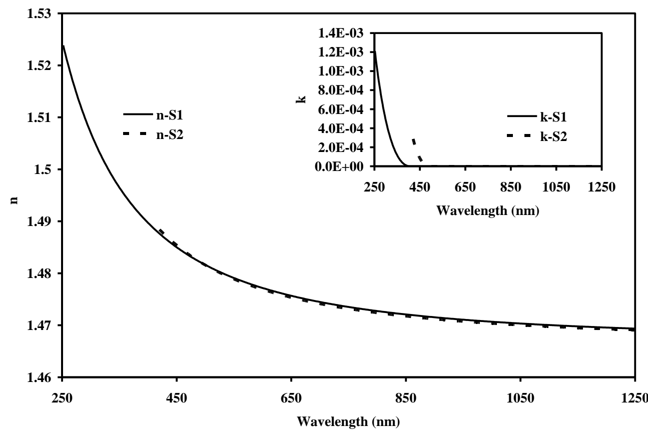

FIG. 7 Refractive index (n) and extinction coefficient (k) for the samples S1 and S2 as a function of wavelength.

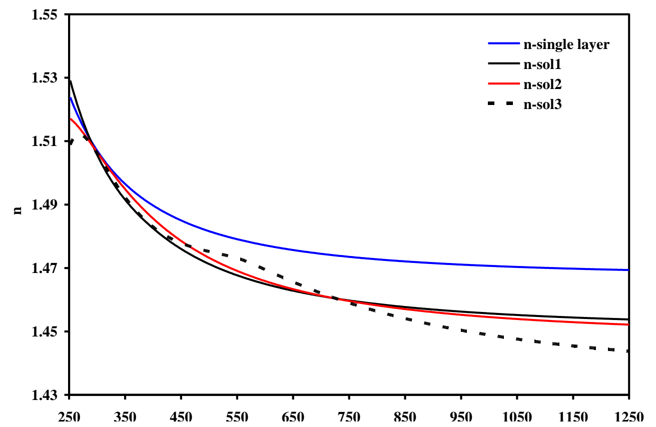

FIG. 9 Refractive index (n) as a function of wavelength, for the SiO_2 layer in the S3 bi-layer, obtained from sol1, sol2 and sol3, compared with the refractive index found for the single S1 SiO_2 layer.

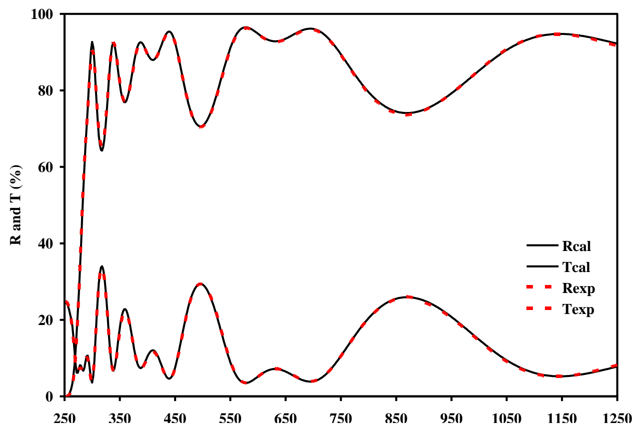

FIG. 8 Experimental and calculated spectra as a function of wavelength, obtained from sol1 for the sample S3.

the single layer determination described in our previous publication [26].

Concerning the SiO_2, its refractive index computed from the three solutions is shown in Figure 9. It can be seen that sol1 and sol2 are similar in terms of the index values. sol3 is slightly different, but should be eliminated since $n = f(\lambda)$ is not a 'physically' acceptable value, and has an oscillatory behavior between 400 nm and 700 nm. However, as can be seen in Figure 9, the index value given by the bi-layer is not exactly the same as that given by the single layer determination. Both indices are the same at $\lambda = 300$ nm ($n = 1.506$), but differ when the wavelength increases. At $\lambda = 1000$ nm, the single layer optimization leads to an index of $n = 1.470$, whereas a bi-layer determination leads to $n = 1.454$. We are convinced that this difference is real. In the case of a bi-layer, the SiO_2 layer is deposited immediately after the Ta_2O_5 layer, and the chamber is already under steady-state conditions (continuous regime). Moreover, a hypothetical transition layer with a thickness in the range 1-5 nm, between the layers of Ta_2O_5 and SiO_2, could also provide an explanation. An index difference of approximately 0.01 is plausible, and would be in agreement with other values reported in the literature [31]–[33].

6 CONCLUSION

In this paper we have determined the complex refractive index of single SiO_2 layers on different substrates and for a bi-layer design. We obtained a similar value of refractive index for single layers, and this could be determined over the range from 250 to 1250 nm using a SiO_2 substrate. The extinction coefficient is no longer detectable at wavelengths above 330 nm, when k is less than $2 \cdot 10^{-4}$. The use of a global algorithm is an efficient means for determining the refractive index of SiO_2 on a bi-layer design including a first layer of Ta_2O_5. The SiO_2 index determinations of single layers and bi-layer show a very small difference (in the 0.01 range) for the visible and NIR wavelength range. When SiO_2 is used in a multilayer stack, we propose to use bi-layer results to determine n, the real part of the complex refractive index, and a single layer on a fused silica substrate to determine k, the imaginary part of the complex refractive index.

7 ACKNOWLEDGEMENTS

This program was supported by the French National Research Agency (ANR, "*Agence National de la Recherche*") (ANR PNANO SEEC).

References

[1] J. A. Dobrowolski, F. C. Ho, and A. Waldorf, "Determination of optical constants of thin film coating materials based on inverse synthesis," Appl. Opt. **22**, 3191–3200 (1983).

[2] J. C. Manifacier, J. Gasiot, and J. P. Fillard,"A simple method for the determination of the optical constants n, k and the thickness of a weakly absorbing thin film," J. Phys. E. Sci. Instrum. **9**, 1002–1004 (1976).

[3] R. Swanepoel, "Determination of the thickness and optical constants of amorphous silicon," J. Phys. E. Sci. Instrum. **16**, 1214–1222 (1983).

[4] R. Swanepoel, "Determining refractive index and thickness of thin films from wavelengh measurements only," J. Opt. Soc. Am. A. **2**, 1339–1343 (1985).

[5] I. Ohlıdal, D. Franta, M. Ohlıdal, and K. N. til, “Optical characterization of nonabsorbing and weakly absorbing thin films with the wavelengths related to extrema in spectral reflectances,” Appl. Opt. **40**, 5711–5717 (2001).

[6] M. Kar, “Errorminimization in the envelope method for the determination of optical constants of a thin film,” Surf. Interface Anal. **42**, 145–150 (2010).

[7] S. Humphrey, “Direct calculation of the optical constants for a thin film using a midpoint envelope,” Appl. Opt. **46**, 4660–4666 (2007).

[8] L. Gao, F. Lemarchand, and M. Lequime, “Exploitation of multiple incidences spectrometric measurements for thin film reverse engineering,” Opt. Express **20**, 15734–15751 (2012).

[9] http://www.heliosoptical.net/Corning_HPFS_7980_Standard_Grade_Fused_Silica.pdf

[10] http://www.ohara-gmbh.com/e/katalog/d_s-lah66_e.html.

[11] R. R. Willey, *Practical Production of Optical Thin Films* (Second Edition, Willey Optical Consultants, Charlevoix, 2012).

[12] P. G. Verly, A. V. Tikhonravov, and M. K. Trubetskov,“Refinement algorithm for the synthesis of inhomogeneous optical coatings,” Appl. Opt. **36**, 1487–1495 (1997).

[13] A. V. Tikhonravov, T. V. Amotchkina, M. K. Trubetskov, R. J. Francis, V. Janicki, J. Sancho-Parramon, H. Zorc, and V. Pervak, “Optical characterization and reverse engineering based on multiangle spectroscopy,” Appl. Opt. **51**, 245–254 (2012).

[14] A. V. Tikhonravov, M. K. Trubetskov, T. V. Amotchkina, G. DeBell, V. Pervak, A. K. Sytchkova, M. L. Grilli, and D. Ristau, “Optical parameters of oxide films typically used in optical coating production,” in Optical Interference Coatings, OSA Technical Digest (Optical Society of America, 2010), paper ThA6.

[15] E. D. Palik,*Handbook of Optical Constants of Solids* (Academic Press, New York, 1985).

[16] B. Mangote, L. Gallais, M. Zerrad, F. Lemarchand, L. H. Gao, M. Commandré, and M. Lequime, “A high accuracy femto-/picosecond laser damage test facility dedicated to the study of optical thin films,” Rev. Sci. Instrum. **83**, 013109 (2012).

[17] H. A. Macleod, *Thin-film Optical Filters* (Institute of Physics Publishing, Bristol and Philadelphia, 2001).

[18] G. E. Jellison, and F. A. Modine, “Parameterization of the optical functions of amorphous materials in the interband region,” Appl. Phys. Lett. **69**, 371–373 (1996).

[19] G. E. Jellison, V. I. Merkulov, A. A. Puretzky, D. B. Geohegan, G. Eres, D. H. Lowndes, and J. B. Caughman, “Characterization of thin film amorphous semiconductors using spectroscopic ellipsometry,” Thin Solid Films **377-378**, 68–73 (2000).

[20] B. v. Blanckenhagen, D. Tonova, and J. Ullmann, “Application of the Tauc-Lorentz formulation to the interband absorption of optical coating materials,” Appl. Opt. **41**, 3137–3141 (2002).

[21] M. Kildemo, R. Ossikovski, and M. Stchakovsky, “Measurement of absorption edge of thick transparent substrates using incoherent reflection model and spectroscopic UV-visible–near IR ellipsometry,” Thin Solid Films **313-314**, 108–113 (1998).

[22] Z. G. Hu, Z. M. Huang, Y. N. Wu, S. H. Hu, G. S. Wang, J. H. Ma, and J. H. Chu, “Optical characterization of ferrelectric $Bi_{3.25}La_{0.75}Ti_3O_{12}$ thin films,” Eur. Phys. J. B. **38**, 431–436 (2004).

[23] R. D. L. Kronig, “On the theory of dispersion of x-rays,” J. Opt. Soc. Am. **12**, 547–556 (1926).

[24] L. Gao, F. Lemarchand, and M. Lequime, “Reverse engineering from spectrophotometric measurements: performances and efficiency of different optimization algorithms,” Appl. Phys. A. **108**, 87–889 (2012).

[25] T. Csendes, “Nonlinear parameter estimation by global optimization - efficiency and reliability,” Acta Cybernetica **8**, 361–370 (1988).

[26] L. Gao, F. Lemarchand, and M. Lequime, “Comparison of different dispersion models for single layer optical thin film index determination,” Thin Solid Films **520**, 501–509 (2011).

[27] K. D. Hendrix, and J. Oliver, “Optical interference coatings design contest 2010: solar absorber and Fabry-Perot etalon,” Appl. Opt. **50**, C286–C300 (2011).

[28] M. Tilsch, and K. Hendrix, “Optical interference coatings design contest 2007: triple bandpass filter and nonpolarizing beam splitter,” Appl. Opt. **47**, C55–C69 (2008).

[29] M. Tilsch, K. Hendrix, and P. Verly, “Optical interference coatings design contest 2004,” Appl. Opt. **45**, 1544–1554 (2006).

[30] A. O’Keefe, and D. A. G. Deacon, “Cavity ring-down optical spectrometer for absorption measurements using pulsed laser sources,” Rev. Sci. Instrum. **59**, 2544–2551 (1988).

[31] I. H. Malitson, “Interspecimen comparison of the refractive index of fused silica,” J. Opt. Soc. Am. **55**, 1205–1209 (1965).

[32] http://refractiveindex.info/

[33] S. Xiong, W. Huang, and Y. Zhang, “The properties of IAD oxide optical coatings,” in Optical Interference Coatings, OSA Technical Digest (Optical Society of America, 2004), paper MB3.